

# 3D Covalent Organic Frameworks of Interlocking 1D Square Ribbons

Yuzhong Liu,<sup>†</sup> Christian S. Diercks,<sup>†</sup> Yanhang Ma,<sup>‡</sup> Hao Lyu,<sup>†</sup> Chenhui Zhu,<sup>§</sup> Sultan A. Alshimri,<sup>||</sup> Saeed Alshihri,<sup>||</sup> and Omar M. Yaghi<sup>\*,†,||</sup>

<sup>†</sup>Department of Chemistry, University of California-Berkeley; Materials Sciences Division, Lawrence Berkeley National Laboratory; and Kavli Energy NanoSciences Institute, Berkeley, California 94720, United States

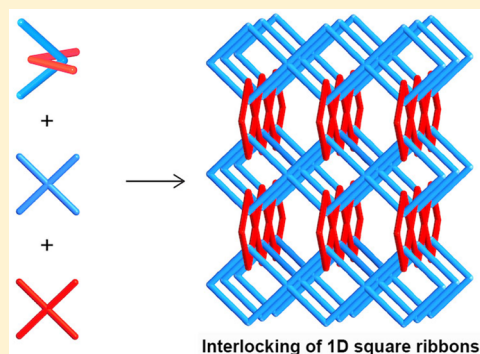
<sup>‡</sup>School of Physical Science and Technology, Shanghai Tech University, Shanghai 201210, China

<sup>§</sup>Advanced Light Source, Lawrence Berkeley National Laboratory, Berkeley, California 94720, United States

<sup>||</sup>UC Berkeley-KACST Joint Center of Excellence for Nanomaterials for Clean Energy Applications, King Abdulaziz City for Science and Technology, Riyadh 11442, Saudi Arabia

## Supporting Information

**ABSTRACT:** A new mode of mechanical entanglement in extended structures is described where 1D organic ribbons of corner-sharing squares are mutually interlocked to form 3D woven covalent organic framework-500, COF-500. Reaction of aldehyde-functionalized tetrahedral Cu(PDB)<sub>2</sub>PO<sub>2</sub>Ph<sub>2</sub> complexes (PDB = 4,4'-(1,10-phenanthroline-2,9-diyl)dibenzaldehyde) with rectangular tetratopic ETTBA (4',4''',4''''',4''''''-(ethene-1,1,2,2-tetrayl)tetrakis-([1,1'-biphenyl]-4-amine)) linkers through imine condensation, yielded a crystalline porous metalated COF, COF-500-Cu, with pts topology. Upon removal of the Cu(I) ions, the individual 1D square ribbons in the demetalated form (COF-500) are held together only by mechanical interlocking of rings, which allows their collective movement to produce a narrow-pore form, as evidenced by nitrogen adsorption and solid-state photoluminescence studies. When exposed to tetrahydrofuran vapor, the interlocking ribbons can dynamically move away from each other to reopen up the structure. The structural integrity of COF-500 is maintained during its dynamics because the constituent square ribbons cannot part company due to spatial confinement imparted by their interlocking nature.



## INTRODUCTION

Molecular weaving of covalent organic frameworks (COFs)<sup>1–3</sup> holds promise for providing solid-state materials capable of dynamics. Such dynamics would be based on movements of mechanically entangled<sup>4–6</sup> threads rather than stretching or bending of chemical bonds. In this context, the term ‘weaving’ is used as a general term for mechanical linkage of 0D and 1D objects to afford extended 2D and 3D structures. The key to designing a woven structure is to control the geometry of the crossing points, the overall connectivity of the linkers, and the angles these components make with respect to each other (Figure 1a and b). Mechanically linked derivatives of almost all synthetically accessible framework topologies can be formed by weaving of threads, interlocking of rings and polyhedra, or, in some cases a combination of these. In principle, access to the wide range of these woven framework structures falls within the realm of reticular chemistry. In this report, we show how 1D open square ribbons of corner-sharing squares, entirely composed of covalently linked organic molecules, can interlock to form extended 3D COFs (Figure 1d). Specifically, linking tetrahedral Cu(PDB)<sub>2</sub> complexes with rectangular tetratopic 4',4''',4''''',4''''''-(ethene-1,1,2,2-tetrayl)tetrakis-([1,1'-biphenyl]-4-amine) (ETTBA) linkers yields the woven COF-500-Cu

with an overall structure based on the platinum sulfide (pts) topology (Figure 2).

The copper ions serve as points of registry that bring together square ribbons in a controlled manner such that they interlock with other ribbons to form a 3D woven framework. We show that COF-500-Cu can be demetalated to produce the purely organic woven form, COF-500, where the individual ribbons are held together only by mechanical interlocking, and that it is possible to remetalate the structure reversibly with full retention of its crystalline order. It is worthy of note that the specific mode of interlocking reported here has not been conceived prior to this report. In COF-500, large degrees of motional freedom, without unzipping of the structure, are observed by vapor sorption and photoluminescence studies. This is attributed to the fact that the individual ribbons of COF-500 can move freely with respect to each other within the confinement of the interlocking rings.

## EXPERIMENTAL SECTION

**Synthesis of Cu(I)-bis[4,4'-(1,10-phenanthroline-2,9-diyl)-dibenzaldehyde] Diphenylphosphinate [Cu(PDB)<sub>2</sub>PO<sub>2</sub>Ph<sub>2</sub>].**

Received: November 13, 2018

Published: December 11, 2018

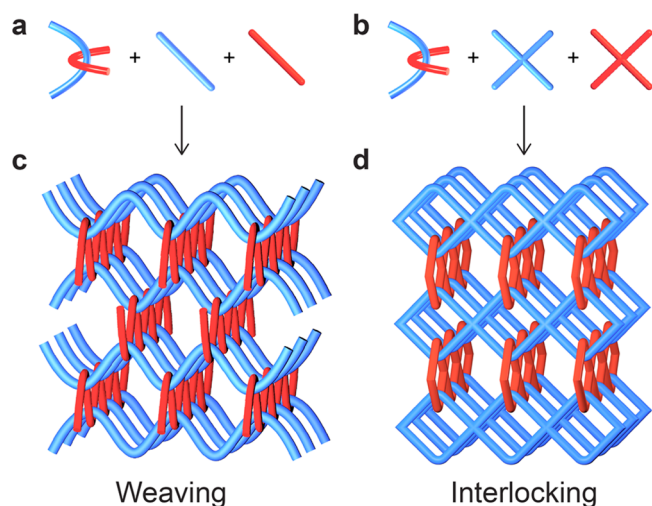


**Figure 1.** Modes of mechanical entanglement in woven COFs. (a) Combination of tetrahedral building blocks encoding for mechanical entanglement with linear struts. (b) Tetrahedral and square-shaped tetratopic linkers encoding for mechanical entanglement. (c) Weaving of 1D threads that cross at regular intervals. (d) Interlocking square ribbons that are held together by entanglement of rings.

Copper(I) diphenylphosphinate (199 mg, 0.710 mmol) was added to a solution of 4,4'-(1,10-phenanthroline-2,9-diyl)dibenzaldehyde (500 mg, 1.29 mmol) in  $\text{CHCl}_3$  (15 mL) and  $\text{CH}_3\text{CN}$  (10 mL) in the glovebox, affording a dark red solution, which was stirred at room temperature for 30 min. The solution was then concentrated under vacuum and further purified by silica column chromatography with a gradient of solvent from 1:100 to 1:10 (v/v) of methanol/dichloromethane. Recrystallization from acetone afforded the analytically pure compound as red crystals (490 mg, 72%).  $^1\text{H NMR}$  (400 MHz,  $\text{dms}\text{-}d_6$ ):  $\delta$  9.68 (s, 4H), 8.83 (d,  $^3J = 7.9$  Hz, 4H), 8.19 (d,  $^3J = 7.9$  Hz, 4H), 8.15 (s, 4H), 7.72 (m, 4H), 7.62 (d,  $^3J = 8.0$  Hz, 8H),

7.43 (m, 6H), 7.07 (d,  $^3J = 8.0$  Hz, 8H). ESI-MS for  $[\text{C}_{52}\text{H}_{32}\text{CuN}_4\text{O}_4]^+$  (calcd 839.17):  $m/z = 839.17$  ( $[\text{M}]^+$ , 100%).

**Synthesis and Activation of COF-500-Cu.** A Pyrex tube measuring  $10 \times 8$  mm (o.d  $\times$  i.d) was charged with  $\text{Cu}(\text{PDB})_2\text{PO}_2\text{Ph}_2$  (17.6 mg, 0.0160 mmol), ETTBA (12.0 mg, 0.0160 mmol), 1 mL of a 1:1 (v/v) 1,2-dichlorobenzene/1-butanol mixture, and 0.1 mL of 9 M aqueous acetic acid. The tube was flash frozen at 77 K (liquid  $\text{N}_2$ ), evacuated to an internal pressure of 50 mTorr, and flame-sealed. Upon sealing, the length of the tube was reduced to 18–20 cm. The reaction was heated at 180 °C for 72 h, yielding a brown solid at the bottom of the tube, which was isolated by centrifugation and washed by Soxhlet extraction with anhydrous tetrahydrofuran (THF) for 12 h. The sample was activated at 85 °C under reduced pressure (50 mTorr) for 12 h. Yield: 21.2 mg, 75.7% based on  $\text{Cu}(\text{PDB})_2\text{PO}_2\text{Ph}_2$ . Anal. Calcd for  $\text{C}_{114}\text{H}_{74}\text{CuN}_8\text{O}_2\text{P}\cdot 6\text{H}_2\text{O}$ : C, 76.47; H, 4.84; N, 6.25. Found: C, 76.43; H, 5.26; N, 6.11. ICP-AES of Cu content: calcd 3.55%; found 3.5%.

## RESULTS AND DISCUSSION

The synthetic strategy to make COF-500 is depicted in Figure 1. Tetrahedral tetratopic  $\text{Cu}(\text{PDB})_2\text{PO}_2\text{Ph}_2$ , an aldehyde-functionalized copper(I)-bisphenanthroline complex salt, was linked with square-planar tetratopic ETTBA through imine bond formation (Supplementary Section S2). In  $\text{Cu}(\text{PDB})_2\text{PO}_2\text{Ph}_2$ , the copper centers preorganize two PDB ligands such that their appended aldehyde functional groups approximate a tetrahedral geometry. The 60° angles between the two points of extension (i.e., aldehyde functionalities) of each PDB ligand are complementary to the 120° angles between the points of extension (i.e., amino functionalities) of ETTBA, thus leading to the formation of four-membered macrocycles (Figure 2a). These macrocycles are covalently linked through the double bonds of ETTBA to yield corner-sharing 1D square ribbons. In each individual ribbon, the phenanthroline ligands comprising the corners of the macrocycles are linked together by copper(I) ions in an embracing

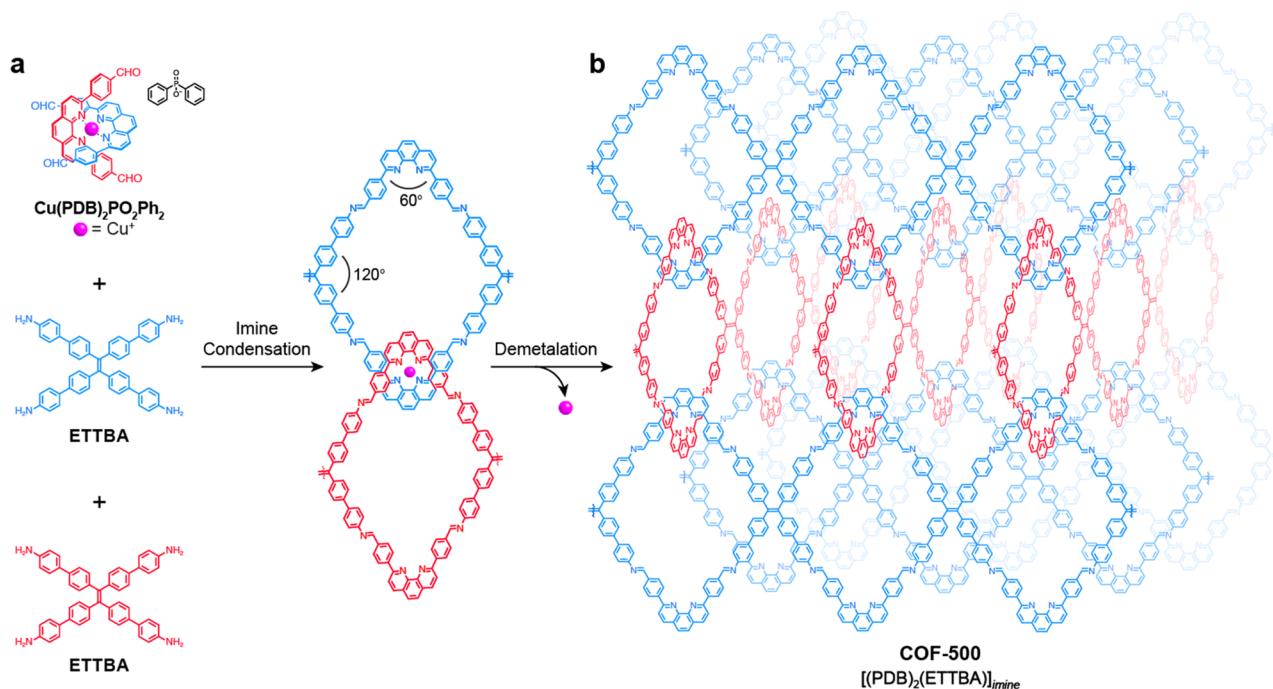


**Figure 2.** Synthetic strategy for the design and synthesis of interlocking 1D square ribbons. COF-500-Cu was constructed from (a)  $\text{Cu}(\text{PDB})_2\text{PO}_2\text{Ph}_2$  and ETTBA to yield interlocking 1D corner-sharing square ribbons connected to each other through copper(I) ions. (b) Upon demetalation an entirely organic extended woven 3D framework, COF-500, with underlying pts topology is formed.

manner. The second set of phenanthroline ligands forms part of an adjacent interlocking ribbon (blue and red, Figure 2a). The entangled ribbons are orthogonal to each other because of the dihedral angle the two phenanthroline ligands of the complex assume, thus yielding a woven 3D framework with an underlying *pts* net, the default net for the linking of tetrahedral and square-planar building units.<sup>7,8</sup>

The synthesis of COF-500-Cu was carried out based on reversible imine bond formation: Equimolar amounts of  $\text{Cu}(\text{PDB})_2\text{PO}_2\text{Ph}_2$  and ETTBA were reacted in a 1:1 (v/v) mixture of 1,2-dichlorobenzene and 1-butanol in the presence of aqueous acetic acid as a catalyst. The reaction mixture was sealed in a Pyrex tube and heated at 180 °C to increase solubility of the starting materials and enhance the reversibility of the reaction. After 3 days, the resulting precipitate was collected and washed by Soxhlet extraction with anhydrous tetrahydrofuran to yield a dark brown crystalline solid, which was found to be insoluble in common organic solvents and water (Supplementary Section S2).

The formation of imine linkages in COF-500-Cu was confirmed by Fourier-transform infrared (FT-IR) spectroscopy and <sup>13</sup>C cross-polarization magic angle spinning (CP-MAS) solid-state NMR spectroscopy (Supplementary Sections S3 and S4). A molecular analogue of COF-500-Cu with a tetraphenylethylene core, (1*E*,1'*E*,1''*E*,1'''*E*)-*N,N',N'',N'''*-(ethene-1,1,2,2-tetrayltetrakis([1,1'-biphenyl]-4',4'-diyl))-tetrakis(1-phenylmethanimine) (ETTP), was used as a model compound (Supplementary Section S2). The disappearance of the C=O stretching vibration at 1695 cm<sup>-1</sup> of the aldehyde functional groups in the FT-IR spectra and the absence of peaks at a chemical shift above 200 ppm in the <sup>13</sup>C CP-MAS NMR solid-state spectrum demonstrate full conversion of the  $\text{Cu}(\text{PDB})_2\text{PO}_2\text{Ph}_2$  aldehyde starting material (Supplementary Section S4). Furthermore, the FT-IR spectrum of COF-500-Cu features characteristic C=N stretching vibrations at 1622 and 1171 cm<sup>-1</sup> (1625 and 1170 cm<sup>-1</sup> for ETTP), corroborating the formation of imine bonds.<sup>1,9,10</sup> These observations support completeness of the reaction and formation of imine bonds between the building blocks to form an extended framework.

Scanning electron microscopy (SEM) micrographs of COF-500-Cu show a homogeneous morphology of rod-shaped crystals with dimensions of approximately 1 μm × 0.2 μm × 0.2 μm (Figure 3a and Supplementary Section S5). After ultrasonic oscillation of the sample in ethanol, individual crystals of COF-500-Cu were dispersed on a copper sample grid for transmission electron microscopy (TEM) studies. 3D electron diffraction tomography (3D-EDT)<sup>11</sup> data of COF-500-Cu were collected by combining specimen tilt and electron-beam tilt in the range of -34.3° to +33.0° with a beam-tilt step of 0.3°. From the acquired data set the 3D reciprocal lattice of COF-500 was constructed and found to have unit-cell parameters of *a* = 21 Å, *b* = 52 Å, *c* = 21 Å, and *V* = 22932 Å<sup>3</sup>, which were used to index reflections observed in both the powder X-ray diffraction (PXRD) pattern and Fourier diffractogram of high-resolution transmission electron microscopy (HRTEM) images (Figure 3b to d and Supplementary Section S6). The unit-cell parameters were optimized further by Pawley refinement of the PXRD pattern to be *a* = 20.0 Å, *b* = 51.9 Å, *c* = 20.0 Å, and *V* = 20760 Å<sup>3</sup>. A structure model of COF-500-Cu was built in Materials Studio 8.0<sup>12</sup> in the orthorhombic space group C222. The calculated PXRD pattern of the modeled structure was found to be in good

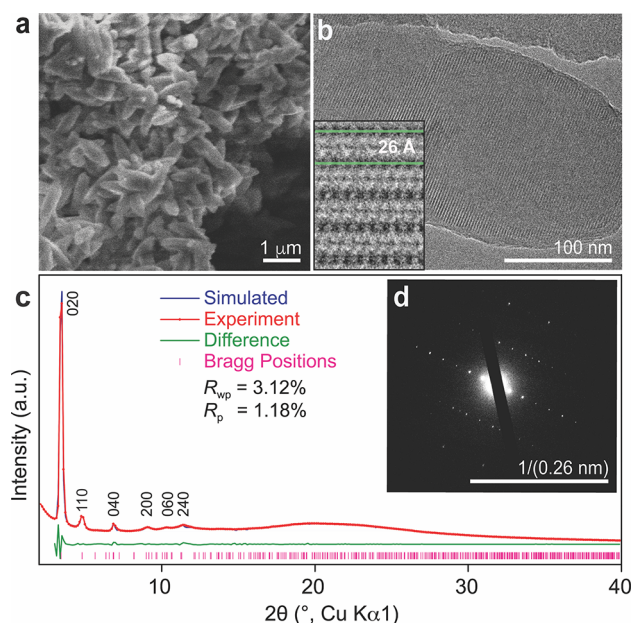


**Figure 3.** Electron microscopy and PXRD studies of COF-500-Cu. (a) Only rod-shaped crystals are observed by SEM, indicating the formation of COF-500-Cu in pure phase. (b) HRTEM image of a single crystal of COF-500-Cu showing lattice fringes with distances of 26 Å (highlighted in the inset). (c) Indexed PXRD pattern of the activated sample of COF-500-Cu (red) and Pawley refinement (blue) of the unit cell from the modeled structure. (d) Selected area electron diffraction pattern acquired from the crystal confirming the single-crystalline nature of the particles.

agreement with the experimental pattern of activated COF-500-Cu.

According to the refined model, COF-500-Cu crystallizes in a *pts* net with tetrahedral building units  $\text{Cu}(\text{PDB})_2\text{PO}_2\text{Ph}_2$  and square-planar ETTBA connected through imine bonds (Figure 4a). Covalently linked 1D square ribbons propagate along the crystallographic *a* (highlighted in blue and cyan) and *c* directions (red and yellow) and are mechanically entangled along the crystallographic *b*-axis (Figure 4b). The Cu–Cu distance within each macrocycle is half of the *b* parameter, 26 Å, which allows for another identical net to reside within the pore (blue/red and cyan/yellow represent the two independent *pts* nets). As the copper centers sit in the 0 1/4 0 and 0 3/4 0 lattice planes in the crystal structure, they are separated by 26 Å viewed along the *c*-axis (Figure 4b), in good agreement with the striped pattern of the lattice fringes observed in the HRTEM image shown in Figure 3b. Overlaying of the derived structure model with the experimentally observed TEM micrograph after applying *P*1 symmetry shows good agreement (Figure 4c). Additional electron density in the pore could be attributed to the presence of counterions.

The copper ions were removed to yield woven COF-500 by heating in a 1 M KCN methanol solution at 75 °C.<sup>1,13</sup> Inductively coupled plasma analysis revealed that more than 99% of the copper ions were removed upon demetalation. The dark color of COF-500-Cu, which arises from the copper–phenanthroline metal-to-ligand charge transfer,<sup>14</sup> disappeared and COF-500 showed a pale yellow color. The crystallinity of COF-500 decreased drastically as compared to its metalated progenitor, indicating spatial rearrangement of the structure and concomitant loss of long-range periodicity. This is expected, as the ribbons in COF-500 experience large degrees

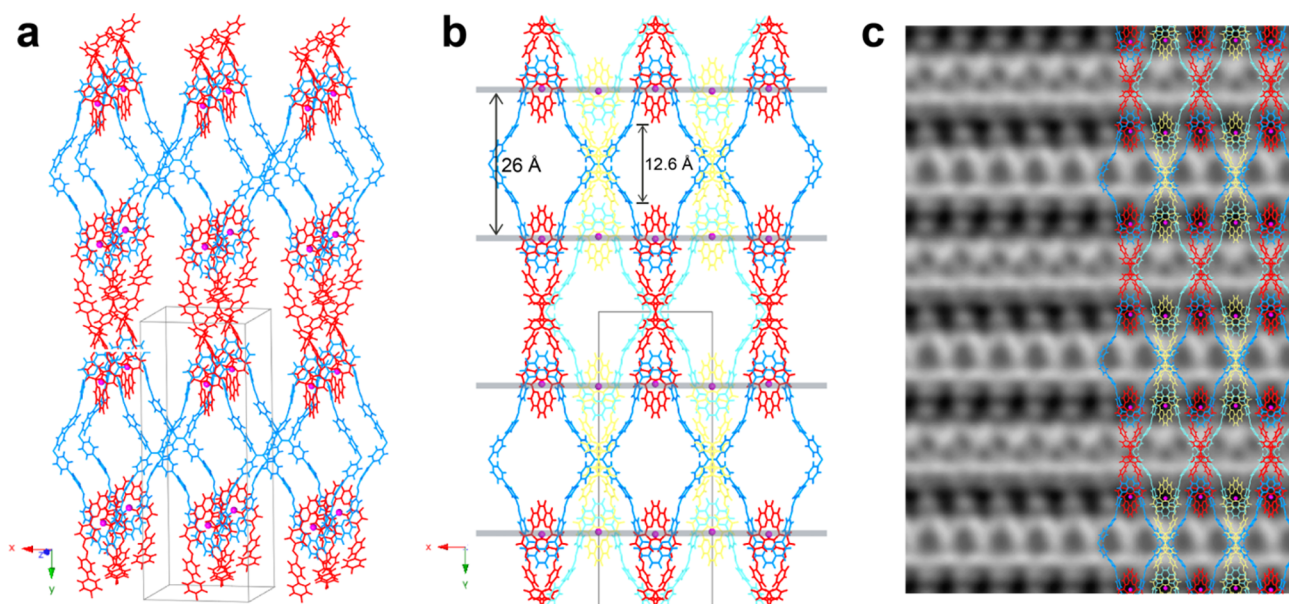


**Figure 4.** Crystal structure of woven COF-500-Cu. (a) One woven framework of COF-500-Cu is constructed from interlocking blue and red 1D square ribbons. The ribbons are entangled through the use of copper(I) ions represented as pink spheres. (b) Representation of the structural model with two entangled woven frameworks viewed along the crystallographic [001] direction revealing that the copper ions are aligned in the  $0\ 1/4\ 0$  and  $0\ 3/4\ 0$  lattice planes separated by 26 Å. (c) Structural model overlaid with a P1 symmetry averaged HRTEM image of COF-500-Cu showing good agreement. Color code: Individual 1D ribbons are depicted in blue, red, cyan, and yellow, respectively. Copper(I) ions are depicted in pink. All counterions are omitted for clarity.

of freedom to move about without the need for breaking or flexing of chemical bonds. The integrity of the overall structure is retained because of the constraints imposed by the mechanical interlocking of the constituents: The FT-IR imine stretching vibration at  $1618\text{ cm}^{-1}$  is consistent with that of the metalated COF-500-Cu ( $1622\text{ cm}^{-1}$ ). In COF-500, the 1D square ribbons are held together by interlocking such that the overall structure remains unaltered. Indeed, upon remetallation of the material by stirring in a solution of acetonitrile/chloroform and  $\text{Cu}(\text{CH}_3\text{CN})_4\text{BF}_4$ , crystalline COF-500-Cu was recovered. The crystallinity and chemical composition of this remetallated framework are identical to the original as-synthesized COF-500-Cu, as evidenced by the complete recovery of the intensity and positions of the reflections in the PXRD pattern as well as the presence of identical vibration bands in the FT-IR spectrum ( $1623\text{ cm}^{-1}$ , Supplementary Section S7). The facile demetallation process indicates that the copper centers in COF-500-Cu are readily accessible due to the openness of the structure.  $\text{N}_2$  gas adsorption isotherms of evacuated samples of both COF-500-Cu and COF-500 were recorded to examine their porosity. The nitrogen isotherm of COF-500-Cu [at 77 K from 0 to 1 bar (1 bar =  $P_0$ )] shows a sharp uptake between  $P/P_0 = 10^{-5}$  and  $10^{-1}$ , a signature feature of microporous materials. The Brunauer–Emmett–Teller (BET) model<sup>15</sup> was applied to the isotherm for  $P/P_0$  between 0.05 and 0.1 to give an apparent surface area of  $S_{\text{BET}} = 352\text{ m}^2\text{ g}^{-1}$ . In contrast, COF-500 exhibited decreased porosity with an  $S_{\text{BET}}$  of only  $155\text{ m}^2\text{ g}^{-1}$  (Figure 5a). Calculation of the pore size obtained from fitting of the two respective isotherms using a nonlinear density functional theory slit pore equilibrium model<sup>16</sup> yielded a definitive pore size of  $12.66\text{ Å}$  for COF-500-Cu, which is in good agreement with the pore size of the crystal structure. In contrast a wider distribution of the pore size from 10 to  $16\text{ Å}$  with a maximum centered at  $12.30\text{ Å}$  was observed for COF-

500, indicating a less well-defined pore system (Figure 5b). This is attributed to the added degrees of freedom and concomitant motional dynamics of the 1D square ribbons upon demetallation.

To obtain additional structural information for COF-500, fluorescence emission spectra before and after demetallation were recorded. The tetraphenylethylene core of ETTBA is known to exhibit aggregation-induced emission.<sup>17–19</sup> When rotation of the phenyl rings along the  $=\text{C}-\text{Ar}$  axes and torsional motions of the  $\text{C}=\text{C}$  bond are unrestricted, both can serve as nonradiative relaxation channels for the decay of the excited state, thus rendering the molecule nonemissive. Once such molecular motion becomes restricted, photoluminescence activity is effectively turned on.<sup>17</sup> Based on the crystal structure of COF-500-Cu there is an ETTBA linker of an adjacent 1D chain located at the center of each macrocycle. Spatial segregation between this ETTBA linker and the phenanthroline corners of the surrounding macrocycle ( $3.4\text{ Å}$  for the closest H–H distance) allows for free rotation of the ETTBA's phenyl rings and thus for quenching of fluorescent emission. Upon demetallation, the phenanthroline corners of neighboring 1D ribbons are free to move about within the constraints of the rigid covalently linked macrocycle of the surrounding ribbons. We believe that, upon removal of the copper(I) ions, the ribbons move closer to the central ETTBA linker in order to maximize van der Waals interactions, thereby restricting the rotation of the phenyl rings and thus affecting aggregation-induced emission. This implies that these ribbons become more packed along the crystallographic  $c$  direction when the material is demetallated, which is consistent with the decrease in uptake observed in  $\text{N}_2$  adsorption studies (Figure 5a).

On the basis of the described sorption and photoluminescence experiments we know that upon demetallation of COF-500-Cu, there is a pronounced structural rearrangement to yield COF-500. To test whether this motion between

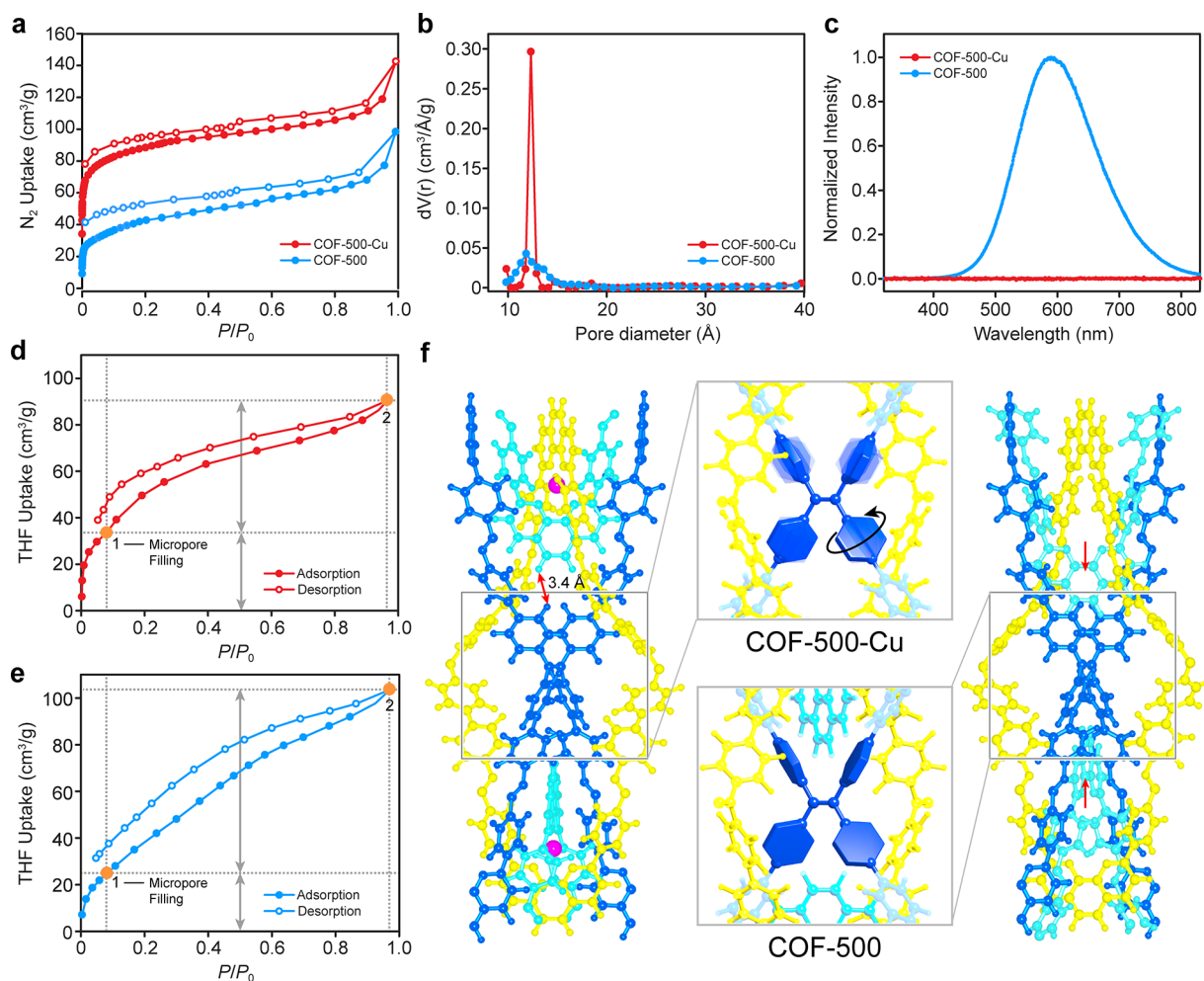


**Figure 5.** Adsorption and solid-state photoluminescence studies of COF-500-Cu and COF-500. (a) Comparison of  $N_2$  sorption isotherms of COF-500-Cu before and after demetalation. Solid and open circles represent the adsorption and desorption branches, respectively. Data of COF-500-Cu and the demetalated framework in this figure are depicted in blue and red, respectively. (b) Pore size distribution calculated from the  $N_2$  sorption isotherms using a nonlinear density functional theory slit pore equilibrium model. (c) Upon excitation at 375 nm, the demetalated framework exhibits an intense emission, while metalated COF-500-Cu is nonemissive. (d and e) THF vapor sorption isotherms of COF-500-Cu and COF-500. (f) Within the boundary of each rigid covalently linked macrocycle (highlighted in yellow), the phenanthroline corners (cyan) are free to move toward the tetraphenylethylene core (blue) upon demetalation. As a result, the motion of the phenyl rings of the tetraphenylethylene core is restricted, thus causing aggregation-induced emission.

adjacent ribbons that yields COF-500 is dynamic, we carried out THF vapor adsorption studies.<sup>20</sup> THF vapor adsorption isotherms were collected for both COF-500-Cu and COF-500 at 283 K. COF-500-Cu shows an uptake with a major step at low partial pressure. The maximum uptake reached at  $P/P_0 = 0.97$  is  $90.5 \text{ cm}^3 \text{ g}^{-1}$  (Figure 5d).<sup>21</sup> For COF-500-Cu, the initial steep uptake saturates at  $P/P_0 = 0.06$  with  $32.0 \text{ cm}^3 \text{ g}^{-1}$  (vs  $P/P_0 = 0.06$  with  $21.9 \text{ cm}^3 \text{ g}^{-1}$  for COF-500, Figure 5e). This is expected, as this uptake is due to filling of the pore that is expected to be partially collapsed in the case of COF-500, thus decreasing its accessible surface area. However, subsequently the adsorption curve of the demetalated framework exhibits a steady linear increase, which suggests opening up of the pores until the maximum uptake of  $103.6 \text{ cm}^3 \text{ g}^{-1}$  is reached at  $P/P_0 = 0.97$ . By taking the density difference between the two materials ( $1680$  and  $1400 \text{ g mol}^{-1}$  for each repeating unit of COF-500-Cu and COF-500, respectively) into consideration, we can roughly approximate the THF adsorption per unit volume. We conclude that in the presence of THF vapor the demetalated framework opens up

to possess 95.3% of the accessible porosity of COF-500-Cu. Thus, upon exposure of COF-500 to THF, the structure adopts an open conformation that likely resembles the structure of COF-500-Cu. The proposed motion in which the 1D ribbons move away from each other in the process of the reopening in the presence of THF can further be supported by additional solid-state photoluminescence studies. After careful dosing of COF-500 with THF on a glass slide, a decrease in emission intensity of approximately 20% as compared to the dry sample is observed (Figure S19, Supplementary Section S29). While this result can only give qualitative information due to limitations in the experimental setup, the decreased intensity nonetheless gives credence to the notion that solvent molecules can diffuse into the less open framework, leading to reopening of the structure and separation of the ribbons such that they are far enough apart from each other to again allow for molecular motion of the phenyl rings of the tetraphenyl ethylene centers. The low emission intensity was retained for at least 10 min even after

surrounding THF evaporated, suggesting strong interactions of THF with the framework.

## CONCLUSION

We report a novel mode of mechanical entanglement in extended structures: interlocking of 1D corner-sharing square ribbons in COF-500-Cu and its demetalated analogue, COF-500. The structure of COF-500-Cu was solved by X-ray powder diffraction and electron microscopy. Upon removal of the copper(I) ions, the 1D ribbons in COF-500 experience large degrees of freedom that allow for their collective movement with respect to one another. The concomitant structural rearrangement is evidenced by decreased nitrogen adsorption and turned-on solid-state photoluminescence. Vapor sorption and photoluminescence studies further showed that exposure to tetrahydrofuran vapor affects dynamic reopening of the framework. The structural integrity of COF-500 is maintained during such dynamic motion, which is credited to constrictions imposed on the movement by the interlocking of its constituents. We anticipate the modular synthesis of COFs combined with the prospect of framework dynamics based on mechanical entanglement to instigate further research on interlocking frameworks.

## ASSOCIATED CONTENT

### Supporting Information

The Supporting Information is available free of charge on the ACS Publications website at DOI: 10.1021/jacs.8b12177.

Synthetic protocols, powder X-ray diffraction analysis, structural modeling, and porosity evaluation of the COFs, as well as details concerning the solid-state NMR and photoluminescence studies (PDF)

## AUTHOR INFORMATION

### Corresponding Author

\*yaghi@berkeley.edu

### ORCID

Yuzhong Liu: 0000-0001-5614-1951

Christian S. Diercks: 0000-0002-7813-0302

Omar M. Yaghi: 0000-0002-5611-3325

### Notes

The authors declare no competing financial interest.

## ACKNOWLEDGMENTS

Financial support for COF research in the O.M.Y. laboratory was provided by King Abdulaziz City for Science and Technology as part of a joint KACST–UC Berkeley collaboration (Center of Excellence for Nanomaterials and Clean Energy Applications). Y.L. was supported by the Philomathia Graduate Student Fellowship in the Environmental Sciences. C.S.D. would like to acknowledge the KAVLI foundation for funding through a KAVLI ENSI graduate student fellowship. Y.M. acknowledges funding support from National Science Foundation of China (NSFC grant no. 21875140). The Advanced Light Source is supported by the Director, Office of Science, Office of Basic Energy Sciences, of the U.S. Department of Energy under Contract No. DE-AC02-05CH11231. The authors acknowledge Ye Zhang and Professor Peidong Yang for solid-state photoluminescence measurement and Dr. Nanette Jarenwattananon and Dr. Hasan Celik for assistance with solid-state NMR studies.

## REFERENCES

- (1) Liu, Y.; Ma, Y.; Zhao, Y.; Sun, X.; Gandara, F.; Furukawa, H.; Liu, Z.; Zhu, H.; Zhu, C.; Suenaga, K.; Oleynikov, P.; Alshammari, A. S.; Zhang, X.; Terasaki, O.; Yaghi, O. M. Weaving of Organic Threads into a Crystalline Covalent Organic Framework. *Science* **2016**, *351*, 365–369.
- (2) Zhao, Y.; Guo, L.; Gandara, F.; Ma, Y.; Liu, Z.; Zhu, C.; Lyu, H.; Trickett, C. A.; Kapustin, E. A.; Terasaki, O.; Yaghi, O. M. A Synthetic Route for Crystals of Woven Structures, Uniform Nanocrystals, and Thin Films of Imine Covalent Organic Frameworks. *J. Am. Chem. Soc.* **2017**, *139*, 13166–13172.
- (3) Liu, Y.; O’Keeffe, M.; Treacy, M. M. J.; Yaghi, O. M. The Geometry of Periodic Knots, Polycatenanes and Weaving from a Chemical Perspective: A Library for Reticular Chemistry. *Chem. Soc. Rev.* **2018**, *47*, 4642–4664.
- (4) Bruns, C. J.; Stoddart, J. F. *The Nature of the Mechanical Bond: From Molecules to Machines*; John Wiley & Sons, 2016.
- (5) Sauvage, J.-P. Transition Metal-containing Rotaxanes and Catenanes in Motion: Toward Molecular Machines and Motors. *Acc. Chem. Res.* **1998**, *31*, 611–619.
- (6) Liu, Y.; Ma, Y.; Yang, J.; Diercks, C. S.; Tamura, N.; Jin, F.; Yaghi, O. M. Molecular Weaving of Covalent Organic Frameworks for Adaptive Guest Inclusion. *J. Am. Chem. Soc.* **2018**, *140*, 16015–16019.
- (7) Yaghi, O. M.; O’Keeffe, M.; Ockwig, N. W.; Chae, H. K.; Eddaoudi, M.; Kim, J. Reticular Synthesis and the Design of New Materials. *Nature* **2003**, *423*, 705–714.
- (8) Delgado-Friedrichs, O.; O’Keeffe, M.; Yaghi, O. M. Taxonomy of Periodic Nets and the Design of Materials. *Phys. Chem. Chem. Phys.* **2007**, *9*, 1035–1043.
- (9) Uribe-Romo, F. J.; Hunt, J. R.; Furukawa, H.; Klock, C.; O’Keeffe, M.; Yaghi, O. M. A Crystalline Imine-linked 3-D Porous Covalent Organic Framework. *J. Am. Chem. Soc.* **2009**, *131*, 4570–4571.
- (10) Zhang, Y.-B.; Su, J.; Furukawa, H.; Yun, Y.; Gandara, F.; Duong, A.; Zou, X.; Yaghi, O. M. Single-crystal Structure of a Covalent Organic Framework. *J. Am. Chem. Soc.* **2013**, *135*, 16336–16339.
- (11) Gemmi, M.; Oleynikov, P. Scanning Reciprocal Space for Solving Unknown Structures: Energy Filtered Diffraction Tomography and Rotation Diffraction Tomography Methods. *Z. Kristallogr. - Cryst. Mater.* **2013**, *228*, 51–58.
- (12) Dassault Systèmes BIOVIA, *Materials Studio 8.0*, Dassault Systèmes, San Diego, 2014.
- (13) Dietrich-Buchecker, C.; Sauvage, J.-P. Templated Synthesis of Interlocked Macrocyclic Ligands: the Catenands. *J. Am. Chem. Soc.* **1984**, *106*, 3043–3045.
- (14) Scaltrito, D. V.; Thompson, D. W.; O’Callaghan, J. A.; Meyer, G. J. MLCT Excited States of Cuprous Bis-phenanthroline Coordination Compounds. *Coord. Chem. Rev.* **2000**, *208*, 243–266.
- (15) Walton, K. S.; Snurr, R. Q. Applicability of the Bet Method for Determining Surface Areas of Microporous Metal-organic Frameworks. *J. Am. Chem. Soc.* **2007**, *129*, 8552–8556.
- (16) Ravikovitch, P. I.; Neimark, A. V. Density Functional Theory Model of Adsorption on Amorphous and Microporous Silica Materials. *Langmuir* **2006**, *22*, 11171–11179.
- (17) Hong, Y.; Lam, J. W. Y.; Tang, B. Z. Aggregation-induced Emission. *Chem. Soc. Rev.* **2011**, *40*, 5361–5388.
- (18) Dalapati, S.; Jin, E.; Addicoat, M.; Heine, T.; Jiang, D. Highly Emissive Covalent Organic Frameworks. *J. Am. Chem. Soc.* **2016**, *138*, 5797–5800.
- (19) Shustova, N. B.; McCarthy, B. D.; Dincă, M. Turn-on Fluorescence in Tetraphenylethylene-based Metal-organic Frameworks: An Alternative to Aggregation-induced Emission. *J. Am. Chem. Soc.* **2011**, *133*, 20126–20129.
- (20) Ma, Y.-X.; Li, Z.-J.; Wei, L.; Ding, S. Y.; Zhang, Y.-B.; Wang, W. A Dynamic Three-Dimensional Covalent Organic Framework. *J. Am. Chem. Soc.* **2017**, *139*, 4995–4998.
- (21) Sing, K. S. W.; Everett, D. H.; Haul, R. A. W.; Moscou, L.; Pierotti, R. A.; Rouquerol, J.; Siemieniewska, T. Reporting

Physisorption Data for Gas/solid Systems with Special Reference to the Determination of Surface Area and Porosity. *Pure Appl. Chem.* **1985**, *57*, 603–619.